

**Cell Reports, Volume 40**

**Supplemental information**

**A central alarm system that gates multi-sensory  
innate threat cues to the amygdala**

**Sukjae J. Kang, Shijia Liu, Mao Ye, Dong-Il Kim, Gerald M. Pao, Bryan A. Copits, Benjamin Z. Roberts, Kuo-Fen Lee, Michael R. Bruchas, and Sung Han**

## Supplementary Figures

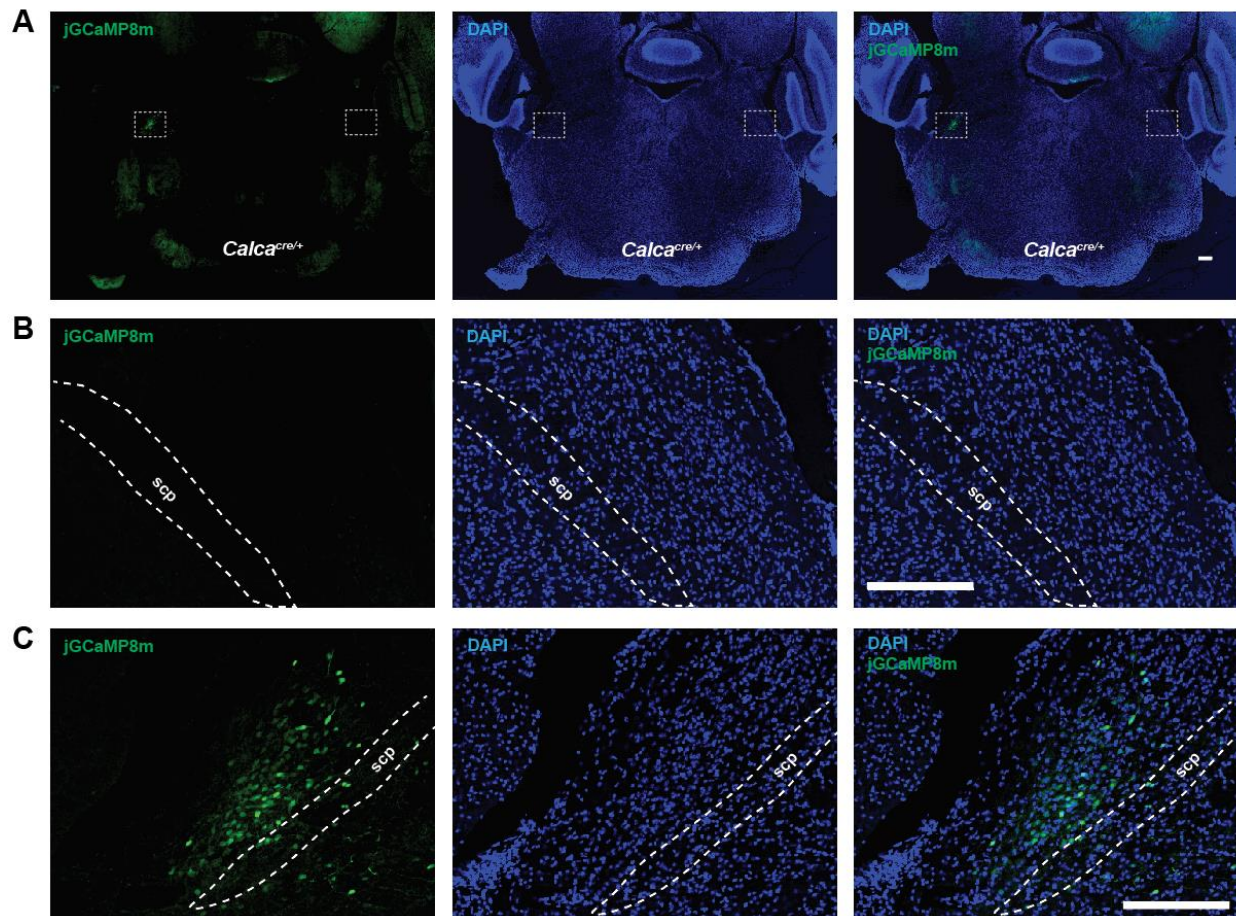


**Figure S1. Confirmation of the GFP signals in *Calca<sup>Cre</sup>* transgenic mouse in the PBel. Related to Figure 1**

(A) Histological images of a *Calca<sup>Cre</sup>* coronal slice containing PBel. The left PBel was injected with AAV-DIO-jGCaMP8m and no action was given to the right PBel. Scale: 200  $\mu$ m.

(B and C) Enlarged histological image of the right (B, no action) and the left PBel (C, with jGCaMP8m expression). Scale: 200  $\mu$ m.

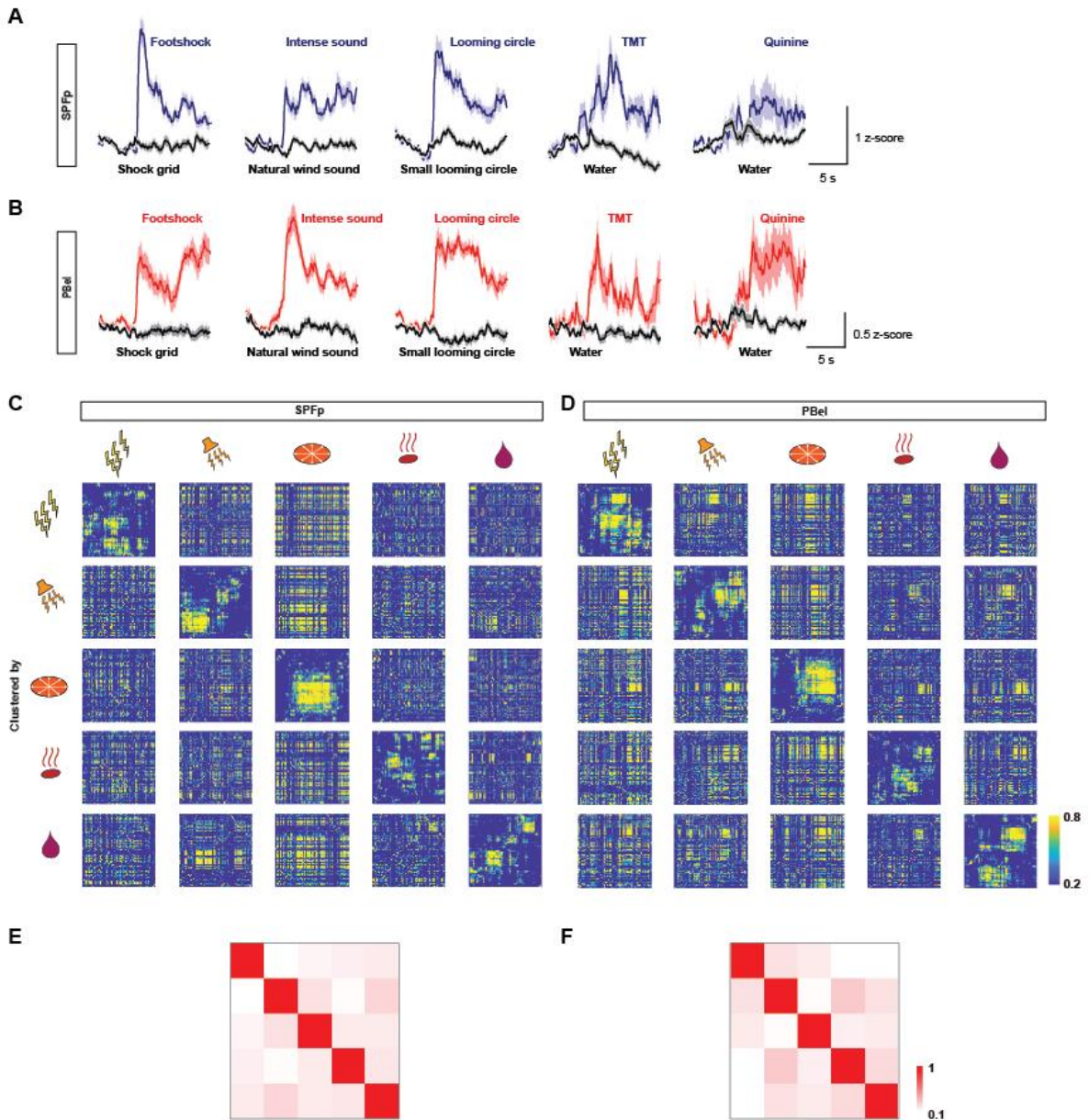


**Figure S2. Multi-sensory threat stimuli recruited different local networks of  $CGRP^{SPFp}$  and  $CGRP^{PBel}$  neurons. Related to Figure 1**

(A and B) Averaged responses of  $CGRP^{SPFp}$  (A) and  $CGRP^{PBel}$  (B) neurons that best respond to five aversive stimuli (blue or red) and those same neurons' responses to control stimuli (black).  $n = 3$  mice per group. Somatosensory: open-circuit shock grid; auditory: 70 dB, 2-sec natural wind sound; visual: small looming circle; olfactory: cotton swab with 10  $\mu$ L water; gustatory: presentation of 10  $\mu$ L water solution to overnight water-restricted mice. Data are presented as mean  $\pm$  SEM.

(C and D) CCM prediction score matrix of 80 SPFp (C) or PBel (D) neurons across five sensory stimuli (somatosensory; auditory; visual; olfactory; gustatory, labeled on the top). Each heatmap incorporates  $80 \times 80$  pairwise prediction scores calculated by CCM. The five matrices presented in the diagonal are the clustergrams for each of the five stimuli produced by the hierarchical clustering algorithm using Pearson

correlation. The icon on the left denotes the identity of the seed heatmap that was used to make the clustergram and determine the order of neurons for the rest four heatmaps in the same row.  $n = 3$  mice per group.

(E and F) CCM manifold similarity matrix of all neuron pairs across five sensory stimuli for SPFp (E) and PBel (F). Heatmaps indicate topological similarity of the manifolds of embedded neural dynamics but do not prove causal interaction. Neurons that were most similar in their dynamics of inputs and outputs were clustered together by hierarchical clustering using Pearson correlation. See Methods section for detailed description of the prediction score heatmap.



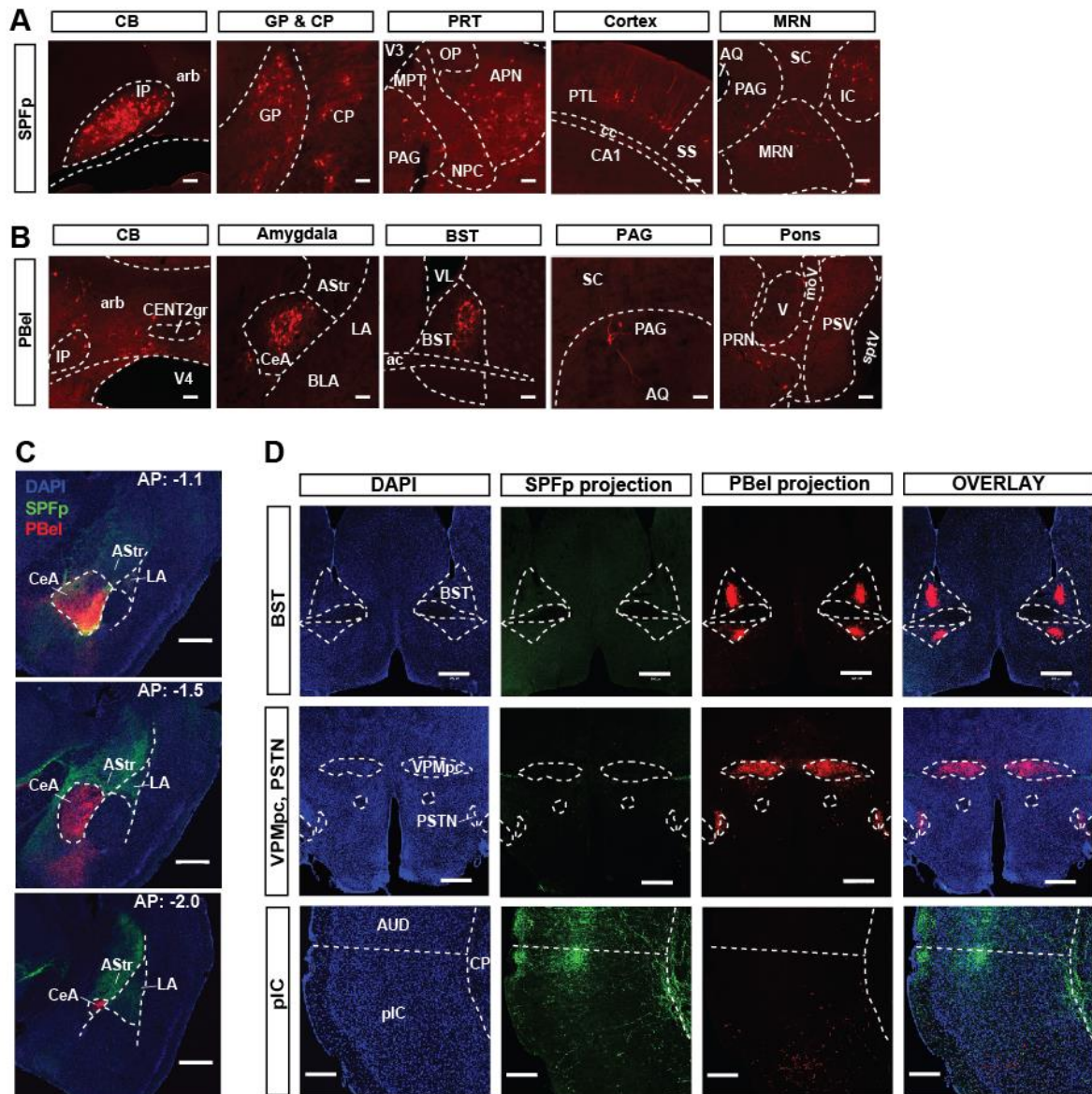


**Figure S3. Additional images of retrograde tracing from  $CGRP^{SPFp}$  and  $CGRP^{PBel}$  neurons and anterograde projections. Related to Figure 2 and 4.**

(A) Example images of brain regions that send inputs to  $CGRP^{SPFp}$  neurons. Scale: 100  $\mu$ m.

(B) Example images of brain regions that send inputs to  $CGRP^{PBel}$  neurons. Scale: 100  $\mu$ m.

(C) Representative histology images from different rostral-caudal axes showing the  $SPFp$  and  $PBel$  projection patterns in the amygdala. Scale: 500  $\mu$ m.

(D)  $CGRP^{SPFp}$  neurons and  $CGRP^{PBel}$  neurons display different projection patterns in other subcortical and cortical areas.  $CGRP^{SPFp}$  neurons project to the auditory cortex and dorsal pIC, while  $CGRP^{PBel}$  neurons project to BNST, VPMpc, PSTN, and ventral pIC. Scale: 500  $\mu$ m for BST and VPMpc/PSTN, 200  $\mu$ m for pIC.

Abbreviations: CENT2gr: Lobule II, granular layer; PTL: parietal association area; SS: somatosensory cortex; moV: motor root of the trigeminal nerve; V: Motor nucleus of trigeminal.

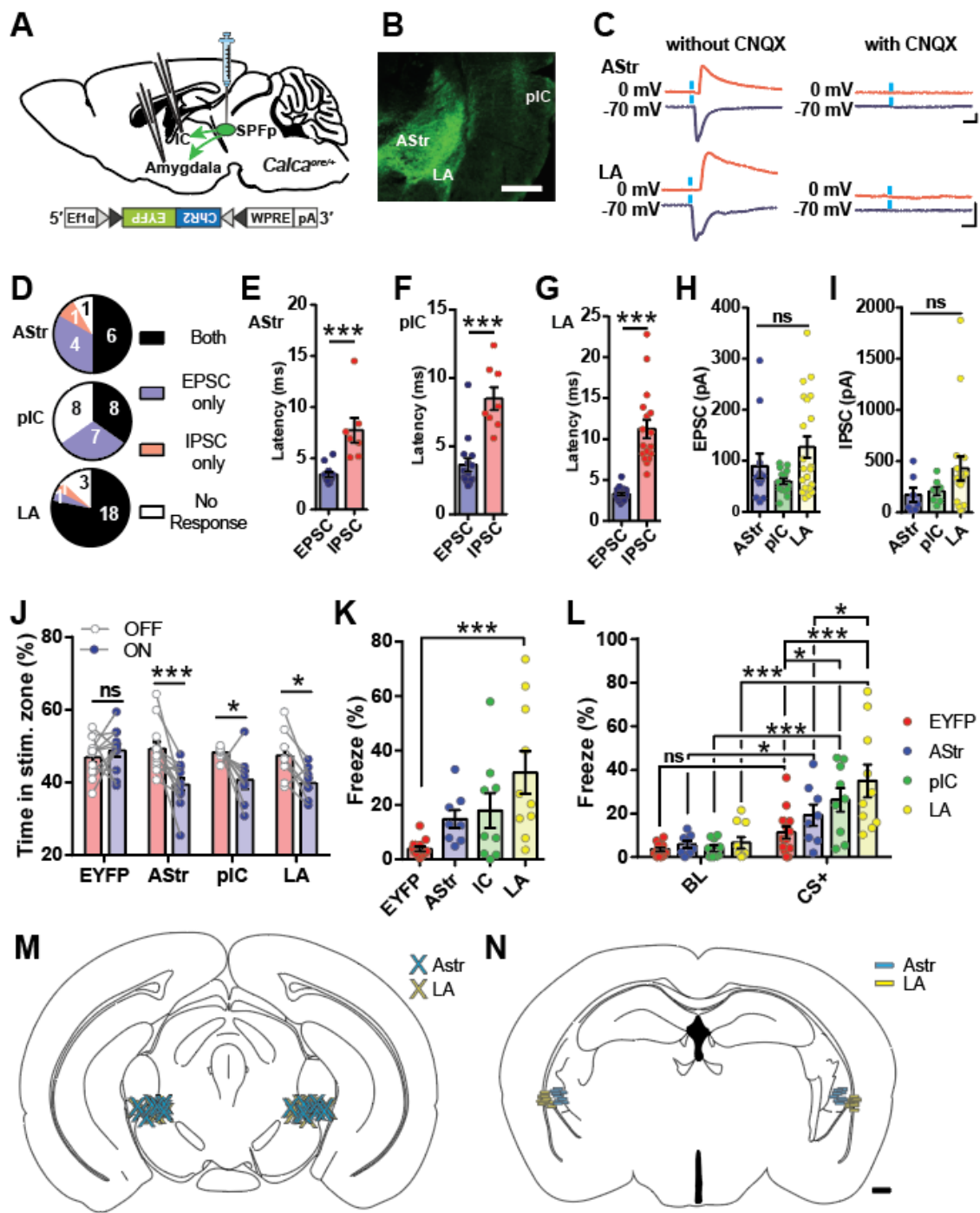


**Figure S4. Characterization of functional downstream of CGRP<sup>SPFp</sup> projection. Related to Figure 4.**

(A) Schematic of slice electrophysiology setup used to characterize the outputs of the CGRP<sup>SPFp</sup> circuit. Cre-dependent ChR2 was expressed in the CGRP<sup>SPFp</sup> neurons.

(B) Representative histology image of the projection regions from CGRP<sup>SPFp</sup> neurons. Scale: 500  $\mu$ m.

(C) Example traces of optically induced EPSC (blue) and IPSC (red) in the AStr (top) and LA (bottom). CNQX application abolished both responses, indicating the existence of glutamatergic synapse. Scale bars: 10 ms and 50 pA.

(D) Proportion of the AStr, pIC and LA cells demonstrating “Both” EPSC and IPSC, “EPSC only”, “IPSC only”, or “No Response”.

(E–H) Latency of EPSC and IPSC onsets following optogenetic stimulation in the AStr (E), pIC (F) and LA (H).

(H) EPSC amplitude following optogenetic stimulation in AStr, pIC, and LA were not significantly different.  $n = 12/7$  (AStr),  $n = 15/7$  (pIC),  $n = 21$  cells/  $9$  mice (LA).

(I) IPSC amplitude following optogenetic stimulation in AStr, pIC, and LA were not significantly different.  $n = 7/7$  (AStr),  $n = 8/7$  (pIC),  $n = 17$  cells/  $9$  mice (LA).

(J) The downstream groups of the  $\text{CGRP}^{\text{SPFP}}$  circuit expressed with ChR2, but not EYFP controls, avoided the chamber paired with terminal photostimulation. EYFP and LA are the same as Figure 4H.  $n = 12$  (EYFP),  $n = 12$  (AStr),  $n = 8$  (pIC) and  $n = 8$  mice (LA).

(K) During the optogenetic threat conditioning test wherein  $\text{CGRP}^{\text{SPFP}}$  terminal photostimulation was used as a US, the LA group displayed higher freezing levels during the context retrieval tests than EYFP controls. EYFP and LA are the same as Figure 6C.  $n = 13$  (EYFP),  $n = 8$  (AStr),  $n = 9$  (pIC) and  $n = 10$  mice (LA).

(L) During the optogenetic threat conditioning test wherein  $\text{CGRP}^{\text{SPFP}}$  terminal photostimulation was used as a US, the LA group displayed higher freezing levels during CS+ of the cue retrieval tests than AStr and EYFP controls. EYFP and LA are the same as Figure 6D.  $n = 13$  (EYFP),  $n = 8$  (AStr),  $n = 9$  (pIC) and  $n = 10$  mice (LA).

(M and N) Schematic mapping of the viral injection (M) and optic fiber implantation sites (N) for the  $\text{CGRP}^{\text{SPFP} \rightarrow \text{Astr}}$  (blue) and  $\text{CGRP}^{\text{SPFP} \rightarrow \text{LA}}$  (yellow) terminal photostimulation experiments.  $n = 8$  (AStr),  $n = 10$  mice (LA). Statistical analyses were performed using two-tailed unpaired t-tests (E, F and G), Kruskal-Wallis one-way ANOVA with post-hoc Dunn’s multiple comparison (H, I and K), and repeated measures two-way ANOVA with post-hoc Sidak’s multiple comparison (J and L). See also Table S5 for statistical details.

\* $P < 0.05$ , \*\*\* $P < 0.001$ . Data are presented as mean  $\pm$  SEM.



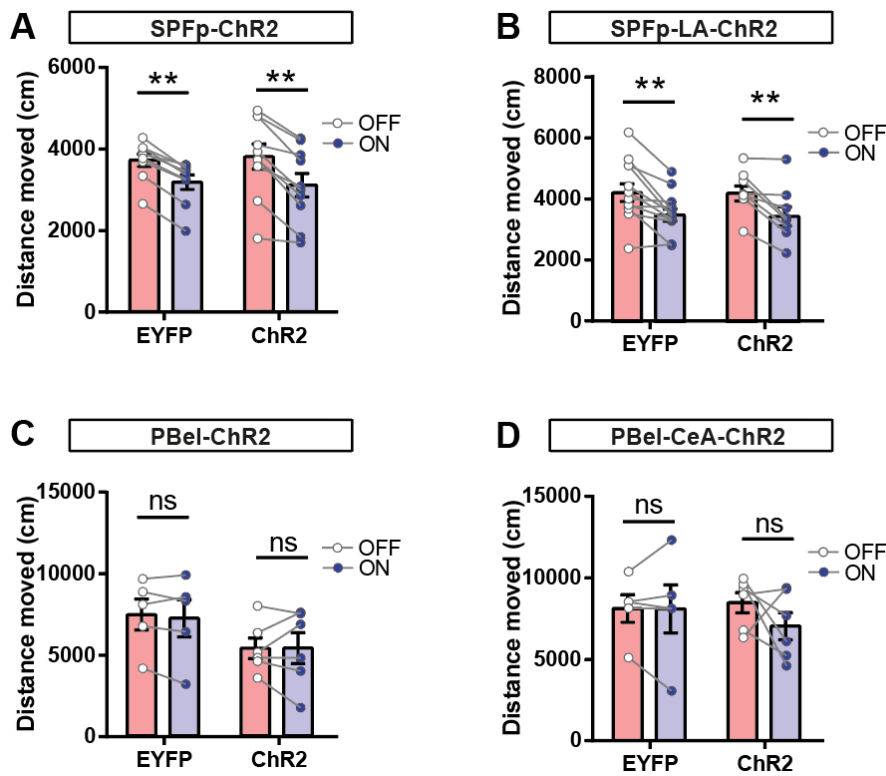


**Figure S5. Locomotion during RTPA tests. Related to Figure 4.**

(A) In the RTPA test with  $\text{CGRP}^{\text{SPFP}}$  cell body photostimulation, EYFP and ChR2 groups showed similar levels of decreases in locomotor activity during laser ON period (last 10 min of the photostimulation period, which is also 20 – 30 min from the start of the experiment) compared to laser OFF period (0 – 10 min from the start of the experiment). Related to Figure 4E.  $n = 9$  (EYFP),  $n = 10$  mice (ChR2).

(B) In the RTPA test with  $\text{CGRP}^{\text{SPFP} \rightarrow \text{LA}}$  terminal photostimulation, EYFP and ChR2 groups showed similar levels of decreases in locomotor activity during laser ON period compared to laser OFF period. Related to Figure 4H.  $n = 12$  (EYFP),  $n = 8$  mice (ChR2).

(C) In the RTPA test with  $\text{CGRP}^{\text{PBel}}$  cell body photostimulation, no significant differences in locomotor activity were observed in the EYFP and ChR2 groups between laser ON and laser OFF periods. Related to Figure 4K.  $n = 5$  (EYFP),  $n = 6$  mice (ChR2).

(D) In the RTPA test with  $\text{CGRP}^{\text{PBel} \rightarrow \text{CeA}}$  terminal photostimulation, no significant differences in locomotor activity were observed in the EYFP and ChR2 groups between laser ON and laser OFF periods. Related to Figure 4N.  $n = 5$  (EYFP),  $n = 6$  mice (ChR2). Statistical analyses were performed using repeated measure two-way ANOVAs with post-hoc Sidak's multiple comparison; see also Table S5 for statistical details.

\*\* $P < 0.01$ . Data are presented as mean  $\pm$  SEM.

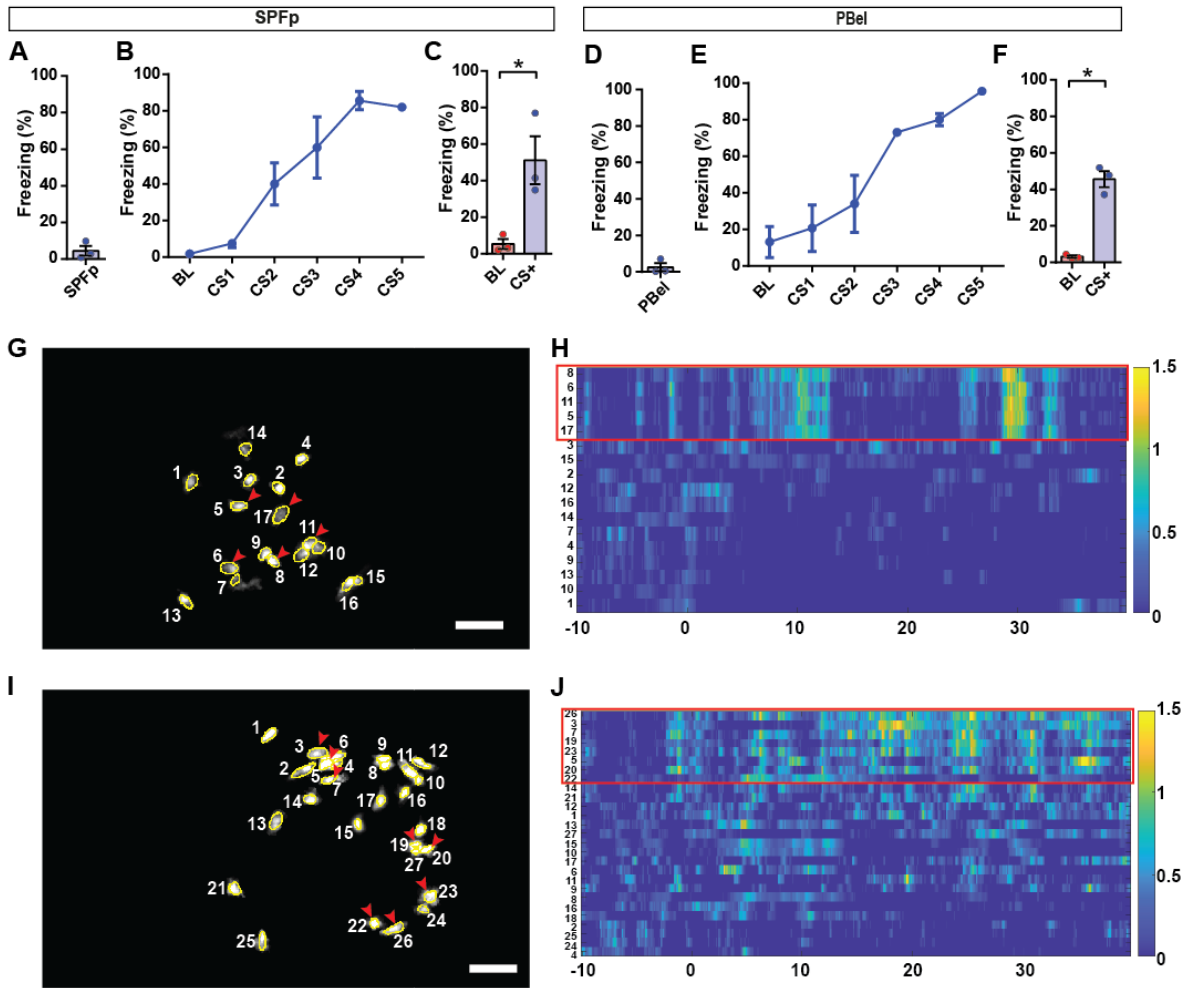


**Figure S6. Animals displayed freezing behaviors during Miniscope single-cell calcium imaging experiments and similar activity patterns were observed in some CGRP<sup>PBel</sup> cells. Related to Figure 6.**

(A–C) Freezing levels during habituation (A), conditioning (B) and cued retrieval tests (C) in the CGRP<sup>SPFP</sup> single-cell calcium imaging experiment.  $n = 3$  mice.

(D–F) Freezing levels during habituation (D), conditioning (E) and cued retrieval tests (F) in the CGRP<sup>PBel</sup> single-cell calcium imaging experiment.  $n = 3$  mice. Statistical analyses were performed using two-tailed paired t-test. See also Table S5 for statistical details.  $*P < 0.05$ . Data are presented as mean  $\pm$  SEM.

(G and I) Example field-of-view of recorded cells (yellow circles) from two mice where jRCaMP8m is expressed in CGRP<sup>PBel</sup> neurons. Image is taken during “Habituation” of the threat conditioning experiment. Red arrowheads indicate the cells showing similar activity patterns that are spatially apart. Scale: 100  $\mu$ m.

(H and J) Heatmap of z-scored CGRP<sup>PBel</sup> single-cell calcium activity during “Habituation”, corresponding to (G and I). X axis denotes time from tone onset (in seconds), y axis denotes cell ID. Red box indicates the activity of red arrowhead cells in (G and I).

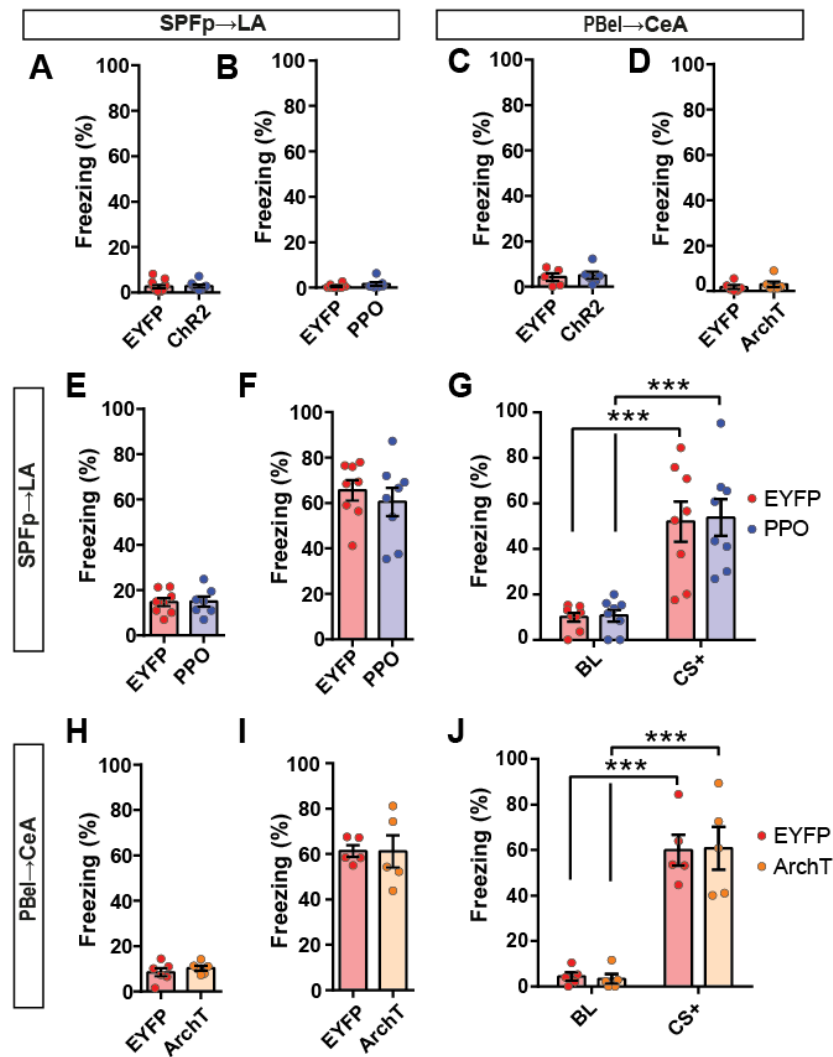


**Figure S7. Animals did not display freezing behaviors during the habituation day (tone presentation only) in the threat conditioning experiments with the  $\text{CGRP}^{\text{SPFP} \rightarrow \text{LA}}$  or  $\text{CGRP}^{\text{PBel} \rightarrow \text{CeA}}$  circuit manipulations and the terminal inhibition of the circuits during the retrieval phase had no effect on freezing behavior. Related to Figure 6.**

(A) Freezing levels during habituation in the  $\text{CGRP}^{\text{SPFP} \rightarrow \text{LA}}$  terminal photostimulation conditioning experiment. Related to Figure 6C and 6D.  $n = 13$  (EYFP),  $n = 10$  mice (Chr2).

(B) Freezing levels during habituation in the  $\text{CGRP}^{\text{SPFP} \rightarrow \text{LA}}$  terminal inhibition threat conditioning experiment. Related to Figure 6E and 6F.  $n = 8$  (EYFP),  $n = 7$  mice (PPO).

(C) Freezing levels during habituation in the  $\text{CGRP}^{\text{PBel} \rightarrow \text{CeA}}$  terminal photostimulation conditioning experiment. Related to Figure 6I and 6J.  $n = 5$  (EYFP),  $n = 6$  mice (Chr2).

(D) Freezing levels during habituation in the  $\text{CGRP}^{\text{PBel} \rightarrow \text{CeA}}$  terminal inhibition threat conditioning experiment. Related to Figure 6K and 6L.  $n = 6$  (EYFP),  $n = 6$  mice (ArchT).

(E–G) Freezing behavior during habituation (E), CGRP<sup>SPFp→LA</sup> circuit inhibition in context (F) and cued retrieval tests (G). n = 8 mice per group.

(H–J) Freezing behavior during habituation (H), CGRP<sup>PBel→CeA</sup> circuit inhibition in context (I) and cued retrieval tests (J). n = 5 mice per group. Statistical analyses were performed using two-tailed unpaired t-tests (A–F, H and I), or repeated measures two-way ANOVA with post-hoc Sidak's multiple comparison (G and J). See also Table S5 for statistical details. \*\*\* $P < 0.001$ . Data are presented as mean  $\pm$  SEM.

**Table S1. Number of cells responding to each unique combination of five different stimulations. For the combinations, 0 and 1 indicate the non-existence and existence of a certain stimulation listed on the leftmost column, respectively. Related to Figure 1.**

Combination	shock	blast	loom	TMT	quinine	Cell count	SPFp	PBel
1	0	0	0	0	0		1	6
2	0	0	1	0	0		1	4
3	0	1	0	0	0		1	4
4	0	1	1	0	0		3	2
5	0	0	0	1	0		0	0
6	0	0	1	1	0		2	1
7	0	1	0	1	0		2	0
8	0	1	1	1	0		2	1
9	0	0	0	0	1		1	4
10	0	0	1	0	1		1	0
11	0	1	0	0	1		1	1
12	0	1	1	0	1		1	3
13	0	0	0	1	1		0	2
14	0	0	1	1	1		0	0
15	0	1	0	1	1		2	3
16	0	1	1	1	1		6	0
17	1	0	0	0	0		2	7
18	1	0	1	0	0		1	6
19	1	1	0	0	0		2	5
20	1	1	1	0	0		6	6
21	1	0	0	1	0		0	1
22	1	0	1	1	0		4	2
23	1	1	0	1	0		1	4
24	1	1	1	1	0		12	6
25	1	0	0	0	1		0	2
26	1	0	1	0	1		1	0
27	1	1	0	0	1		4	3
28	1	1	1	0	1		4	2
29	1	0	0	1	1		4	1
30	1	0	1	1	1		4	2
31	1	1	0	1	1		3	1
32	1	1	1	1	1	8	1	



**Table S2. Accumulative percentage of cells responding to each unique modality. Related to Figure 1.**

<b>% of cells</b>	<b>SPFp</b>	<b>PBel</b>
shock	70	61.25
blast	72.5	52.5
loom	70	45
TMT	62.5	31.25
quinine	50	31.25

**Table S3. Number of input cells of CGRP<sup>SPFP</sup> neurons. Related to Figure 2.**

Brain Region	# of cells					
	Mice #	1	2	3	4	5
<b>CB</b>		159	247	46	137	58
<b>SPV</b>		27	24	64	27	2
<b>RN</b>		121	78	28	40	27
<b>VN</b>		93	38	14	26	8
<b>Pons</b>		204	141	218	166	71
<b>MRN</b>		249	167	310	244	244
<b>IC</b>		287	76	656	187	257
<b>SC</b>		795	503	611	675	547
<b>PAG</b>		95	115	77	108	79
<b>PRT</b>		175	62	175	117	60
<b>SNr</b>		125	81	103	249	100
<b>VTA</b>		62	41	28	31	26
<b>HY</b>		245	91	171	134	299
<b>Amy</b>		86	108	18	21	22
<b>CTX</b>		367	203	234	327	216
<b>CP</b>		197	162	100	75	79
<b>GP</b>		197	238	93	47	77
<b>TH</b>		202	144	408	317	234
<b>BST</b>		3	5	0	6	3
<b>CN</b>		18	3	0	4	2
<b>HPF</b>		4	0	32	0	2
<b>SI</b>		87	54	35	38	80
<b>Not in graph</b>		31	23	24	33	31
<b>Total</b>		3829	2604	3445	3009	2524

**Table S4. Number of input cells of CGRP<sup>PBel</sup> neurons. Related to Figure 2.**

Brain Region	# of cells						
	Mice #	1	2	3	4	5	6
CB		13	67	23	6	15	28
SPV		6	32	44	14	20	53
RN		5	33	109	51	31	62
VN		12	52	5	20	17	42
Pons		6	22	80	3	0	8
MRN		0	13	22	5	2	12
IC		0	10	65	22	1	0
SC		0	16	23	2	2	9
PAG		9	47	29	15	7	24
PRT		3	0	0	0	0	0
SNr		0	0	0	0	0	1
VTA		0	1	0	0	9	7
HY		16	72	108	43	36	53
Amy		17	77	114	64	64	138
CTX		1	3	5	0	3	4
CP		0	12	0	0	0	0
GP		0	0	1	1	0	0
TH		1	4	1	0	0	1
BST		2	15	31	14	13	21
CN		2	5	5	0	0	2
Not in graph		0	0	0	0	1	16
Total		93	485	669	260	226	482

**Table S5. Summary of statistical analysis. Related to all Figures.**

Uploaded as separate excel file.